Beyond the Resolution Limit: Diffusion Parameter Estimation in Partial Volume

Zach Eaton-Rosen[1(✉)], Andrew Melbourne[1], M. Jorge Cardoso[1], Neil Marlow[2], and Sebastien Ourselin[1]

[1] Translational Imaging Group, Centre for Medical Image Computing, University College London, London, UK
rmapzea@ucl.ac.uk
[2] Academic Neonatology, EGA UCL Institute for Women's Health, London, UK

Abstract. Diffusion MRI is a frequently-used imaging modality that can infer microstructural properties of tissue, down to the scale of microns. For single-compartment models, such as the diffusion tensor (DT), the model interpretation depends on voxels having homogeneous composition. This limitation makes it difficult to measure diffusion parameters for small structures such as the fornix in the brain, because of partial volume. In this work, we use a segmentation from a structural scan to calculate the tissue composition for each diffusion voxel. We model the measured diffusion signal as a linear combination of signals from each of the tissues present in the voxel, and fit parameters on a per-region basis by optimising over all diffusion data simultaneously. We test the proposed method by using diffusion data from the Human Connectome Project (HCP). We downsample the HCP data, and show that our method returns parameter estimates that are closer to the high-resolution ground truths than for classical methods. We show that our method allows accurate estimation of diffusion parameters for regions with partial volume. Finally, we apply the method to compare diffusion in the fornix for adults born extremely preterm and matched controls.

1 Introduction

Diffusion imaging is a vital tool for probing the microstructure of *in-vivo* tissue. Parametric models of diffusion offer an informative way to summarise the information from many different b-values and gradient directions. The model parameters are often averaged over a region, under the reasonable assumption that tissue within a structure will have similar diffusion properties. This approach works well in large regions, where we can erode a probabilistic segmentation to obtain voxels that are fully within the tissue. But, the diffusion parameters within structures such as the fornix—a narrow white matter structure, surrounded by cerebrospinal fluid—might not be measured well by this approach, especially at typical diffusion resolutions [1]. Because of the large scale of diffusion MRI voxels relative to the fornix many, and perhaps all, voxels will contain partial volume. This partial volume affects the ability to interpret

© Springer International Publishing AG 2016
S. Ourselin et al. (Eds.): MICCAI 2016, Part III, LNCS 9902, pp. 605–612, 2016.
DOI: 10.1007/978-3-319-46726-9_70

the parameters of diffusion parameter models. For instance, the size of the fornix may confound parameter estimation by introducing varying amounts of partial volume in different subjects or at different timepoints (for example, due to atrophy). In order for the measured diffusion parameters to accurately represent microstructure, we must remove the confound of partial volume.

In this work, we extend the calculation of a region's parameters to include information from all voxels in the region *during* the model-fitting, instead of fitting voxel-wise and then averaging. While there has been work on eliminating the contribution of free water to diffusion parameter estimates [2], our proposed approach directly estimates the diffusion parameters of all tissue types within the image, without relying on *a priori* diffusion models or values. In the proposed framework, we use a probabilistic segmentation as weights for canonical diffusion signals, optimised for each segmentation class or tissue (we use the terms interchangeably). The modelled signal in a voxel is calculated as a weighted sum of each tissue present in the voxel, where the weights are given by the segmentation probabilities (which represent the proportion of each tissue type present).

We first validate the method on *in-vivo* diffusion data from the Human Connectome Project [3]. By using such high-resolution data, we can measure diffusion parameters in the fornix directly, using hand-drawn regions of interest. By downsampling this data, we simulate a more typical diffusion acquisition, and are able to test whether our approach retrieves the correct parameter values. After validating our approach, we apply it to adults born extremely preterm, comparing the diffusion within the fornix to that of term-born controls. The comparison is interesting as the patient group has pervasive differences in brain morphology and function, including memory (associated with the fornix).

This framework presented is similar to [4] in its use of multi-modal imaging to make a diffusion mixture model. This work differs in that there is no requirement of multiple shells of diffusion data, an important advantage for using this method in older data.

2 Methods

2.1 Theory

In this work we attempt to measure diffusion parameters from below the resolution at which they were obtained. If we imagine a voxel at a higher resolution (for example, the T_1-weighted scan) being downsampled to a lower resolution (the diffusion scans), the proportion of the tissue in a voxel of diffusion space will be reduced. Even in a best case scenario, the probability of there being at least a threshold T% of the tissue within a voxel depends on the position of the tissue relative to the voxel borders. Our approach eliminates the dependence of measured parameters on the precise voxel boundaries, by using all diffusion information within the region of interest.

In diffusion MRI, the diffusion of water within is summarised with a mathematical model. Within a given voxel, the water diffusion from several microstructural environments is measured together. A voxel's signal, S, in the diffusion

tensor (DT) model, is given by:

$$\frac{S}{S_0} = e^{-b\mathbf{g}^T\mathbf{D}\mathbf{g}} \tag{1}$$

where S_0 is the diffusion signal with zero diffusion weighting, b are the b-values, $\mathbf{g}$ are the gradient directions and $\mathbf{D}$ is the second-rank diffusion tensor.

In our approach, we aim to obtain $\mathbf{D}$ for each of the k tissue classes (in the case of the fornix, white matter and CSF). In a given voxel, we model the signal as being represented as a weighted sum of each of the tissue classes that are present:

$$S = S_0 \sum_{j=1}^{k} p_j e^{-b\mathbf{g}^T\mathbf{D}_j\mathbf{g}} \tag{2}$$

$\mathbf{D_j}$ is now the diffusion tensor for a given region or tissue. The p_j are non-negative, and constrained between 0 and 1. The $\mathbf{D_j}$ are unknown parameters that are optimised to best fit the data. This is a mixture-model approach, that generates the diffusion parameter estimates for the entire volume simultaneously, instead of per voxel. For the case of two tissue classes, this reduces to the signal model in [1].

In order for a single DT to represent the diffusion properties in different voxels, we must account for different orientation in different parts of the same tissue. Conventionally, we would use the same b-matrix for each voxel in the image. However, we are mainly interested in orientationally-independent measurements, such as the fractional anisotropy (FA). In this work, we redefine the gradient-directions for each voxel, so that the principal directions of all voxels in the image align. The gradient directions at each voxel are calculated by first, performing a tensor-fit to the voxel and establishing $\mathbf{v}_1$ and $\mathbf{v}_2$, the first and second eigenvectors of $\mathbf{D}$. We then calculate the rotation matrix R such that $\mathbf{v}_1$ and $\mathbf{v}_2$ align with [1,0,0] and [0,1,0]. Our vector for the i^{th} voxel then becomes $\mathbf{g}_i = R\mathbf{g}$.

After calculating principal diffusion directions in every voxel, and the S_0, with a weighted-least-squares tensor fit, we initialise a $3 \times k$ matrix with identical diffusivities in each of the tissue classes. At each iteration of the optimisation, we calculate the signal for the entire volume simultaneously, before the $3\,k$ diffusion parameters are updated. We fit using Matlab 2014b, using non-linear optimisation [5].

3 Experiments and Results

3.1 MRI Data

To test the proposed approach, we use data from the HCP [3]. The diffusion data has a resolution of $1.25^3\,\mathrm{mm}^3$, with 108 volumes with b $\approx 1000\,\mathrm{s.mm}^{-2}$ (including reference volumes). The T_1-weighted MRI is at resolution $0.70^3\,\mathrm{mm}^3$.

For the experiments on adult subjects, we collected MRI data at 19 years of age from 15 adolescents. Eight (4 Male) of these were born extremely preterm (fewer than 26 weeks completed gestation) and seven (3 Male) were recruited as matched controls. We acquired 3D T1-weighted volume at 1 mm isotropic resolution (TR/TE = 6.78/3.06 ms) for segmentation and diffusion MRI with the following characteristics: four b-values at b = (0, 300, 700, 2000) s.mm^{-2} with n = (4, 8, 16, 32) directions respectively at TE=70 ms ($2.5 \times 2.5 \times 3.0$ mm). For the fitting, we discarded the highest shell of b-values. All data was acquired using a Philips 3T Achieva. For the segmentations, we manually drew the fornix on a T_1-weighted segmentation and also labelled the surrounding tissue using multi-atlas label propagation and fusion [6] based on the Neuromorphometrics, Inc. labels.

3.2 Validating Method Using HCP Data

We used the high resolution of the HCP data to determine pseudo ground-truth values for diffusion parameters in the column, the crus and the body of the fornix. Each of these regions is hand-drawn onto the subject's T_1-weighted MRI. We downsample the segmentation from categorical labels into a probabilistic diffusion segmentation, where the probabilities represent fractions of the tissue in that diffusion voxel. We varied the downsampling to achieve voxels of isotropic dimension from 1.25 mm to 3.5 mm. In order to use HCP data as a model for a more typical diffusion acquisition, we adjust it in the following ways. We added rician noise to the downsampled data, to bring the data to a clinically realistic SNR. We only use one shell of the acquired data, to ignore effects that are not modelled with the DT. For each experiment, we used a subset of the 108 volumes. We tested the performance of our algorithm with between 12 and 60 of these volumes.

We compare three approaches for analysing average parameter values:

M1 For each region, we identify voxels where the membership to that region is above the threshold and average their values.
M2 We resample the downsampled DWI to high-resolution HCP space before fitting the DT model and, again, averaging the values for each region. For this, we use 7th-order b-splines, as recommended in [7].
M3 (proposed): We calculate parameter values for each region, explicitly accounting for partial volume. The p are given by downsampling labels from the T_1-weighted segmentation into diffusion space.

3.3 Results

In Fig. 1 we test approach M1. As the threshold changes, so do the results for the classical approach. At a resolution of 2 mm isotropic, all fornix tissue has partial volume, so we would be unable to use a threshold of 90 % even at this good resolution. However, as we decrease the threshold, increasing the voxel dimension results in decreasing FA, as CSF partial volume contaminates the

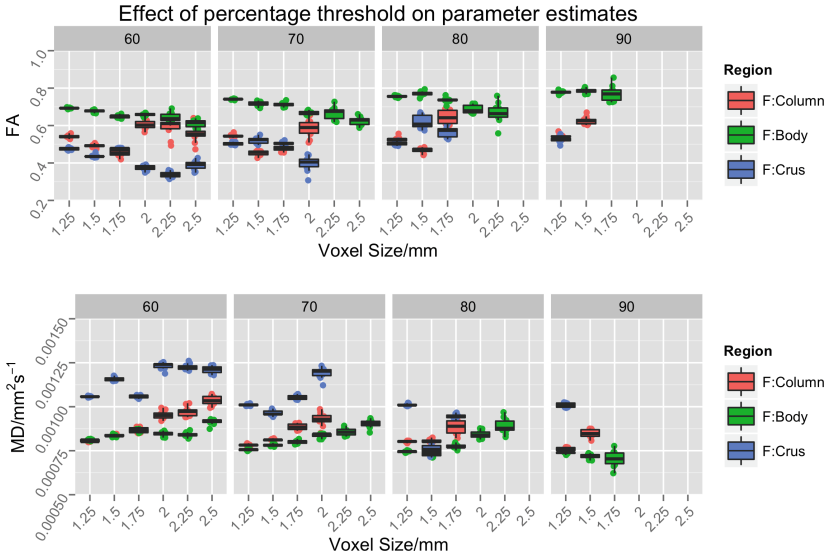

Fig. 1. In this graph, we see the effect of downsampling the resolution (x axis) on parameter estimates from a threshold-based approach. As the voxel dimension increases, the parameter estimation is less reliable and at some point stops, as there are no more supra-threshold voxels to sample. The choice of the threshold will influence the measured parameter value

estimates. For the body of the fornix, the measured FA decreases by up to 13 % by changing the thresholding, and when downsampled to 2.5 mm, the measured FA is up to 25 % lower than the pseudo-gold-standard.

In approach M2, we use the segmentation at the HCP resolution. After downsampling the data and adding noise, we interpolate the diffusion data back to the HCP resolution in order to fit the diffusion tensor and average the results over the ROI. These results are displayed in Fig. 2. The measured diffusion parameters diverge from their 'true' values as we interpolate data of lower resolution. With no downsampling, the values of nearby white matter, the column and the crus of the fornix are similar. However, as the downsampling increases, the FA estimates decrease due to the partial volume. This means that parameter values that should be similar are diverging because of local surroundings.

With the proposed method, the FA in the column and crus of the fornix is constant (Fig. 2). The body of the fornix has an increasing FA. The mean diffusivities are more constant in the proposed method than with the classical.

3.4 Comparison of Preterm-Born and Term-Born Young Adults

We compare fornix DTI parameters as calculated with M2 (upsampling DWI to T_1-space and fitting the tensor) and M3 (proposed) in Fig. 3. The MD in the fornix is higher in general for the classical approach compared to ours. In the

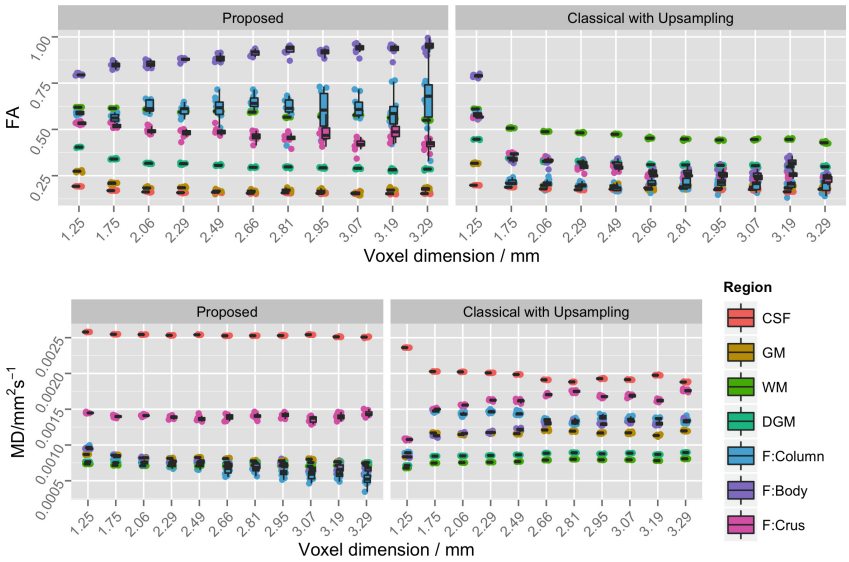

Fig. 2. In our method (left), the diffusion parameters in the fornix are fairly consistent with downsampling. While the results for larger regions match the classical approach, we improve for the fornix. We present the results for a thresholding approach *with* prior upsampling of the data (right). The results here, for diffusion parameters of the fornix, show a divergence of the diffusion parameter readings depending on their surrounding tissue. The scale factor is the factor by which we've downsampled the volume. In these experiments, we used 12 diffusion readings, 2 of which were reference volumes

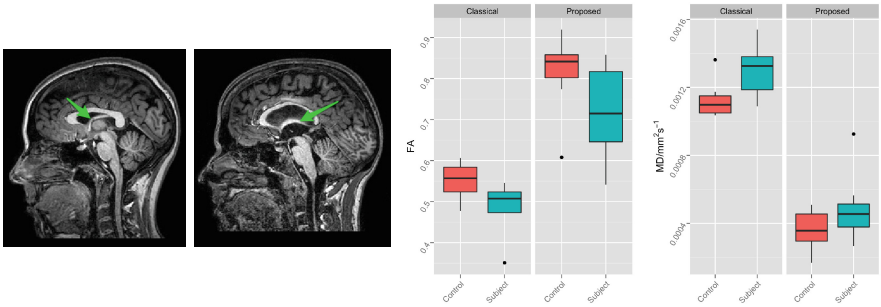

(a) Control (b) Subject (c)

Fig. 3. In a–b the fornix is highlighted with an arrow in a control and a preterm subject. The preterm-born subject has noticeable abnormalities in the corpus callosum, and enlarged ventricles. In c, we display the measured parameters using our proposed approach vs the classical.

classical approach, there is a significant difference in the MD with the subject group having higher MD ($p \leq 0.0005$), which does not appear with the proposed method. Both approaches measure higher mean FA in the control group, but neither is significant when accounting for multiple comparisons. The fitting took less than a minute for each subject.

4 Discussion

Our method achieves consistent and accurate parameter estimates for small regions in partial volume. Although interpolating data reveals some details that are hidden at low resolution [7], interpolation of downsampled HCP data biased the results of the measured diffusion parameters in the fornix. FA values in all parts of the fornix tended to be underestimated and diverged from FA estimates in other white matter regions. This means that the local surroundings of the fornix biased the diffusion results, which our method was able to address.

There is promise in using this approach in subject groups, such as the preterm-born young adults in this study. Our approach reduces the impact of partial volume on measuring the properties of the fornix. The lower MD we measured for both subjects and controls is in accord with this. The higher FA values suggest that we are able to measure the diffusion in the highly-anisotropic region of the fornix with less impact from the surrounding cerebrospinal fluid. While this is not a conclusive result, due to the small number of subjects, it is a promising sign. There is some evidence from both methods that preterm-born adults have lower FA in the fornix than controls, which is congruent with the known result that preterm-born adults exhibit lower FA values in white matter.

While there are a range of biophysical compartment models in use in diffusion imaging, most of these rely on multi-shell data to fit compartments in each voxel, or else have to heavily restrict the available parameters. We circumvent this by fitting on a per-tissue basis, by using information from a structural segmentation.

Another way to calculate diffusion parameters would be using super-resolution techniques. Image Quality Transfer [8] uses a machine-learning approach to super-resolve the diffusion data from diffusion tensors. For this particular method, it is unclear how generalisable the approach is without high-resolution training data from each scanner in use. Our validation only used 12 diffusion volumes, and no training data, which renders the method suitable to past datasets.

We show that it is feasible and possible to estimate diffusion parameters for regions that are small on the scale of diffusion MRI. In large, contiguous regions we achieved the same results as for the classical approach, of thresholding and averaging. We used the fornix as a region of interest to show that our approach was able to recover diffusion parameter estimates consistently, when the classical approach failed. Although results were good in the fornix, the model would have to be extended significantly to cope with geometry such as crossing fibres.

The presented approach achieves close-to gold-standard results with minimal processing time and requirements for the diffusion acquisition. This is because

we aggregate data from all voxels in which a particular tissue is present, even in part. This type of approach fits conceptually with more sophisticated, multi-compartment models, in its representation of a voxel's signal as coming from multiple sources.

In this work, we proposed a method to extract diffusion tensor parameters from tissue that has partial volume. We have validated the method using high-quality data from the HCP, and applied it in a new cohort of clinical interest.

Acknowledgments. We would like to acknowledge the MRC (MR/J01107X/1), the National Institute for Health Research (NIHR), the EPSRC (EP/H046410/1) and the National Institute for Health Research University College London Hospitals Biomedical Research Centre (NIHR BRC UCLH/UCL High Impact Initiative BW.mn.BRC10269). This work is supported by the EPSRC-funded UCL Centre for Doctoral Training in Medical Imaging (EP/L016478/1).
HCP data were provided by the HCP, WU-Minn Consortium (PIs: David Van Essen and Kamil Ugurbil; 1U54MH091657) funded by NIH and Wash. U.

References

1. Metzler-Baddeley, C., O'Sullivan, M.J., Bells, S., Pasternak, O., Jones, D.K.: How and how not to correct for CSF-contamination in diffusion MRI. NeuroImage **59**(2), 1394–1403 (2012)
2. Pasternak, O., Sochen, N., Gur, Y., Intrator, N., Assaf, Y.: Free water elimination and mapping from diffusion MRI. Magn. Reson. Med. **62**(3), 717–730 (2009)
3. Van Essen, D.C., Ugurbil, K., Auerbach, E., Barch, D., Behrens, T.E.J., Bucholz, R., Chang, A., Chen, L., Corbetta, M., Curtiss, S.W., Della Penna, S., Feinberg, D., Glasser, M.F., Harel, N., Heath, A.C., Larson-Prior, L., Marcus, D., Michalareas, G., Moeller, S., Oostenveld, R., Petersen, S.E., Prior, F., Schlaggar, B.L., Smith, S.M., Snyder, A.Z., Xu, J., Yacoub, E.: The human connectome project: a data acquisition perspective. NeuroImage **62**(4), 2222–2231 (2012)
4. Eaton-Rosen, Z., Cardoso, M.J., Melbourne, A., Orasanu, E., Bainbridge, A., Kendall, G.S., Robertson, N.J., Marlow, N., Ourselin, S.: Fitting parametric models of diffusion MRI in regions of partial volume. In: Proceedings of SPIE, Medical Imaging: Image Processing, vol. 9784 (2016)
5. Coleman, T.F., Li, Y.: An interior trust region approach for nonlinear minimization subject to bounds. SIAM J. Optim. **6**(2), 418–445 (1996)
6. Cardoso, M.J., Modat, M., Wolz, R., Melbourne, A., Cash, D., Rueckert, D., Ourselin, S.: Geodesic information flows: spatially-variant graphs and their application to segmentation and fusion. IEEE Trans. Med. Imaging **34**, 1976–1988 (2015)
7. Dyrby, T.B., Lundell, H., Burke, M.W., Reislev, N.L., Paulson, O.B., Ptito, M., Siebner, H.R.: Interpolation of diffusion weighted imaging datasets. NeuroImage **103**, 202–213 (2014)
8. Alexander, D.C., Zikic, D., Zhang, J., Zhang, H., Criminisi, A.: Image quality transfer via random forest regression: applications in diffusion MRI. In: Golland, P., Hata, N., Barillot, C., Hornegger, J., Howe, R. (eds.) MICCAI 2014, Part III. LNCS, vol. 8675, pp. 225–232. Springer, Heidelberg (2014)